Stromal Expression of MMP-13 Is Required for Melanoma Invasion and Metastasis

Paola Zigrino[1], Isolde Kuhn[1], Tobias Bäuerle[2], Jan Zamek[1], Jay W. Fox[3], Susanne Neumann[1], Alexander Licht[4], Marina Schorpp-Kistner[4], Peter Angel[4] and Cornelia Mauch[1]

Tumor invasion and metastasis of malignant melanoma have been shown to require proteolytic degradation of the extracellular environment achieved primarily by enzymes of the matrix metalloproteinases (MMP) family. We have earlier shown that increased enzyme activity is localized at the border of tumor cells and the adjacent peritumoral connective tissue, emphasizing the importance of tumor-stroma interactions in the regulation of MMP activity. To confirm the role of stroma-derived MMP-13 in the invasion process, we investigated the invasiveness of melanoma cells upon intradermal injection in mice with complete inactivation of MMP-13. Tumor growth was significantly impaired in mmp-13$^{-/-}$ mice and most significant at early time points as compared with wild-type littermates. Moreover, metastasis to various organs was reduced to 17.6 *vs* 30% in lungs, 2.9 *vs* 30% in the liver. Strikingly, ablation of MMP-13 completely abrogated formation of metastasis in the heart (0 *vs* 40%). Notably, decreased tumor growth in mmp-13$^{-/-}$ mice was associated with reduced blood vessel density. In addition, decreased blood vessel permeability in the tumors was measured by magnetic resonance imaging of tumor-bearing animals. These data suggest an important role of MMP-13 in tumor growth and an unexpected role in organ-specific metastasis of melanoma cells.

INTRODUCTION

Degradation and/or remodeling of matrix components is one of the events necessary for melanoma cell invasion through tissues and it is accomplished by the concerted action of different proteases. The best-characterized proteases in this process are the matrix metalloproteinases (MMP). In normal tissues, basal expression and activity of MMPs is almost absent. However, under certain physiological as well as in pathological conditions, different factors have been shown to modulate the expression and activity of MMPs, such as contact of the cells with extracellular matrix (ECM) components and the release of cytokines and growth factors (Itoh *et al.*, 1995; Wandel *et al.*, 2000; Loffek *et al.*, 2005). Also, several growth factors (EGF, PDGF, bFGF, VEGF) and cytokines (for example, IL-1, IL-6, TNF-α, TGF-β) are secreted by tumor-infiltrating inflammatory cells as well as by tumor or stromal cells and can modulate *de novo* synthesis of MMPs.

The proposed role of MMPs in tumor invasion is mainly based on the observation of high-level expression of distinct MMPs in invasive malignant tumors (reviewed by Westermarck and Kahari, 1999). It is widely accepted that collagenases play an important role in the cleavage of the interstitial fibrillar collagens of types I, II, and III. Therefore, degradation of collagenous ECM by these MMPs is likely to be essential for invasion of malignant cells and tumor-associated neovascularization. For instance, mice lacking MMP-7 revealed reduction in intestinal tumorigenesis (Wilson *et al.*, 1997) and MMP-2-deficient mice show reduced angiogenesis and tumor progression (Itoh *et al.*, 1998).

Several recent investigations have shown that in various human carcinomas expression of MMPs is localized to both tumor and stromal cells at the invading margin of the tumor, providing a mechanism for highly concerted degradation of ECM. In human melanoma, MMP-1 protein has been localized to stromal fibroblasts adjacent to the tumor cells, whereas tumor cells and fibroblasts distant to the tumor site stained negative for MMP-1 (Airola *et al.*, 1999). A different distribution has been shown for the expression of MMP-14 and 13. Immunohistochemical analysis of melanoma tissue has shown that MMP-2 and MMP-14 and their inhibitors TIMP-1 and -2 are detected within the tumor and the surrounding stroma (Kurschat *et al.*, 2002). Although in breast carcinoma, MMP-13 was found to be expressed primarily by stromal fibroblasts, in squamous cell carcinoma, it was predominantly confined to the tumor cells (Airola

[1]Department of Dermatology and Center for Molecular Medicine (CMMC), University of Cologne, Cologne, Germany; [2]Department of Medical Physics in Radiology, Heidelberg, Germany; [3]Department of Microbiology, University of Virginia, Virginia, USA and [4]Division of Signal Transduction and Growth Control, Heidelberg, Germany

Correspondence: Dr Cornelia Mauch, Department of Dermatology, University of Cologne, Kerpener Str. 62, Cologne 50931, Germany. E-mail: Cornelia.Mauch@uk-koeln.de

et al., 1997). As MMP-1 is not produced in the murine system, MMP-13 and MMP-14 most likely represent the main collagenases in mice.

Mouse MMP-13 has been demonstrated to play an important role in skeletal development (Stickens *et al.*, 2004). During tumor growth and progression of breast cancer a prominent upregulation of mouse MMP-13 was observed in the stroma (Lafleur *et al.*, 2005). However, skin homeostasis and cutaneous wound healing are independent of MMP-13 likely due to functional compensation by MMP-8 (Hartenstein *et al.*, 2006).

Using mice carrying a complete inactivation of the mmp-13 gene, we have addressed the role of stroma-derived MMP-13 for the development of melanoma grafts *in vivo*. Further, we demonstrated that development and metastasis of melanoma *in vivo* depends greatly on the expression of MMP-13 in the peritumoral area. The impaired tumor growth and metastasis in MMP-13-deficient mice may be attributed at least partially to reduced tumor angiogenesis.

RESULTS
MMP-13 is expressed in endothelial cells of B16F1 grafts *in vivo*
Under physiological conditions, expression of MMP-13 is almost absent in murine skin (Madlener *et al.*, 1998; Hartenstein *et al.*, 2006). In agreement with these data, analysis of MMP-13 transcripts in unaffected murine skin shows no amplification product from RNA extracted from complete skin upon reverse transcription (RT)–PCR amplification (Figure 1a). A strong induction of MMP-13 mRNA transcripts was observed in B16 tumors developing in wild-type (WT) animals 10 days post-tumor cell injection, whereas expression of MMP-13 transcripts was completely absent in B16 tumors generated in knockout animals. These data indicate that expression of MMP-13 is not induced in tumor

cells but rather in the tumor-activated stromal compartment. The expression of the second main collagenase in mice, MMP-14 was similar for WT and mmp13$^{-/-}$ animals (Figure 1b).

Immunohistological examination of the B16F1 tumors raised in WT mice show expression of MMP-13 mainly in the stromal areas proximal to melanoma cell invasion (Figure 2a, s, stroma; t, tumor). Small MMP13-positive local spots were also observed in the peripheral tumor mass (Figure 2, tumor) and in few intratumoral cells. Tumor cells were identified by staining for the tyrosinase-related protein-1 (Figure 2a, TRP-1). These data together with the transcript analysis suggest an importance for stromally derived MMP-13 for melanoma growth *in vivo*. Confocal analysis depicted expression of MMP-13 in the cytoplasm of CD31-positive cells with a polarized distribution toward the vessel lumen where it is likely to be secreted (Figure 2b, A′). Expression of MMP-13 was found in smooth muscle actin-positive cells (B and B′; SMA, red) surrounding the vessel, whereas no MMP-13 expression was observed in tumor-infiltrating neutrophils (Figure 2b, C and C′). Interestingly, some but not all CD68-positive macrophages also showed a strong cytoplasmic staining for MMP-13 (Figure 2b; D and white arrows in D′).

Host-derived MMP-13 is important for the growth and metastasis of melanoma *in vivo*
To analyze the influence of stroma-derived MMP-13 expression in peritumoral areas on the development of melanoma *in vivo*, we have grafted B16F1 melanoma cells by intradermal injection into the flank of WT and mmp-13$^{-/-}$ animals. Tumor growth was measured as a function of time. Measurable B16F1 melanomas were detected as early as at day 2 post-injection and reached an average size of 600 mm^3 10 days post-injection (Figure 3a). In contrast, depletion of stromal MMP-13 significantly inhibited tumor growth. In MMP-13 null mice, melanomas were only visible and measurable at day 4 and had a strikingly reduced average size of 300 cm^3 after 10 days as compared with injected littermate controls (Figure 3a).

In parallel, we have analyzed metastasis formation 9 days post-injection by RT–PCR analysis of mRNA from different isolated organs for the expression of GFP transcripts solely expressed from GFP-tagged melanoma cells. This analysis revealed a consistent reduction in the overall metastasis to the lungs, liver, and brain of the mmp-13$^{-/-}$ animals (Figure 3b). Comparison of WT and mmp-13$^{-/-}$ animals showed reduced metastases in mmp-13$^{-/-}$ mice as compared with control littermates in 17.6 *vs* 30% of the lungs, 2.9 *vs* 30% in the liver, and 11.8 *vs* 30% in the brain. The most significant difference was associated with metastasis to the hearts. No metastasis was found in hearts from mmp-13$^{-/-}$ as compared with WT animals, where melanoma cells infiltrated 40% of the hearts.

Figure 1. Matrix metalloproteinases (MMP)-13 is produced by tumor-activated stroma. B16F1-GFP melanoma cells were injected intradermally in wild-type (WT) or knockout MMP-13 mice (mmp-13$^{-/-}$) and allowed to grow for 10 days. (**b**) Primary tumors grown in three different WT and mmp-13$^{-/-}$ mice, numbered from 1 to 3, or normal unaffected skin (**a**) were prepared. RNA was isolated from all tissues and reverse transcription–PCR was performed as described in ''Materials and Methods'' section. GFP amplification was used to identify of B16F1 melanoma cells, whereas S26 was used as loading control. Note that MMP-13 transcripts were amplified in tumors from WT animals but not from those grown in mmp-13$^{-/-}$ animals. MMP-14 was amplified in both extracts.

Lack of MMP-13 results in reduced tumor growth and invasion due to inhibition of angiogenesis but not of the inflammatory reaction
MMP-13 expression was observed in CD31 and some CD68 positive cells (Figure 2, A′ and D′, arrows) suggesting that
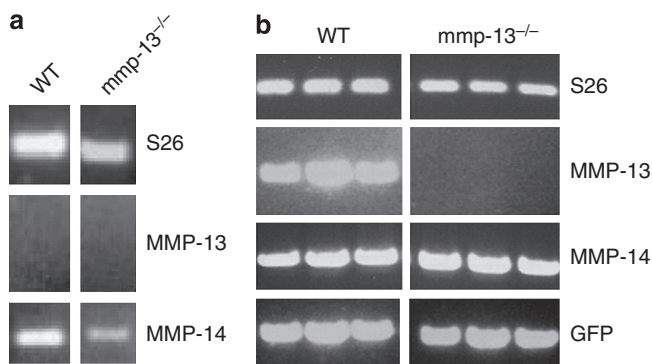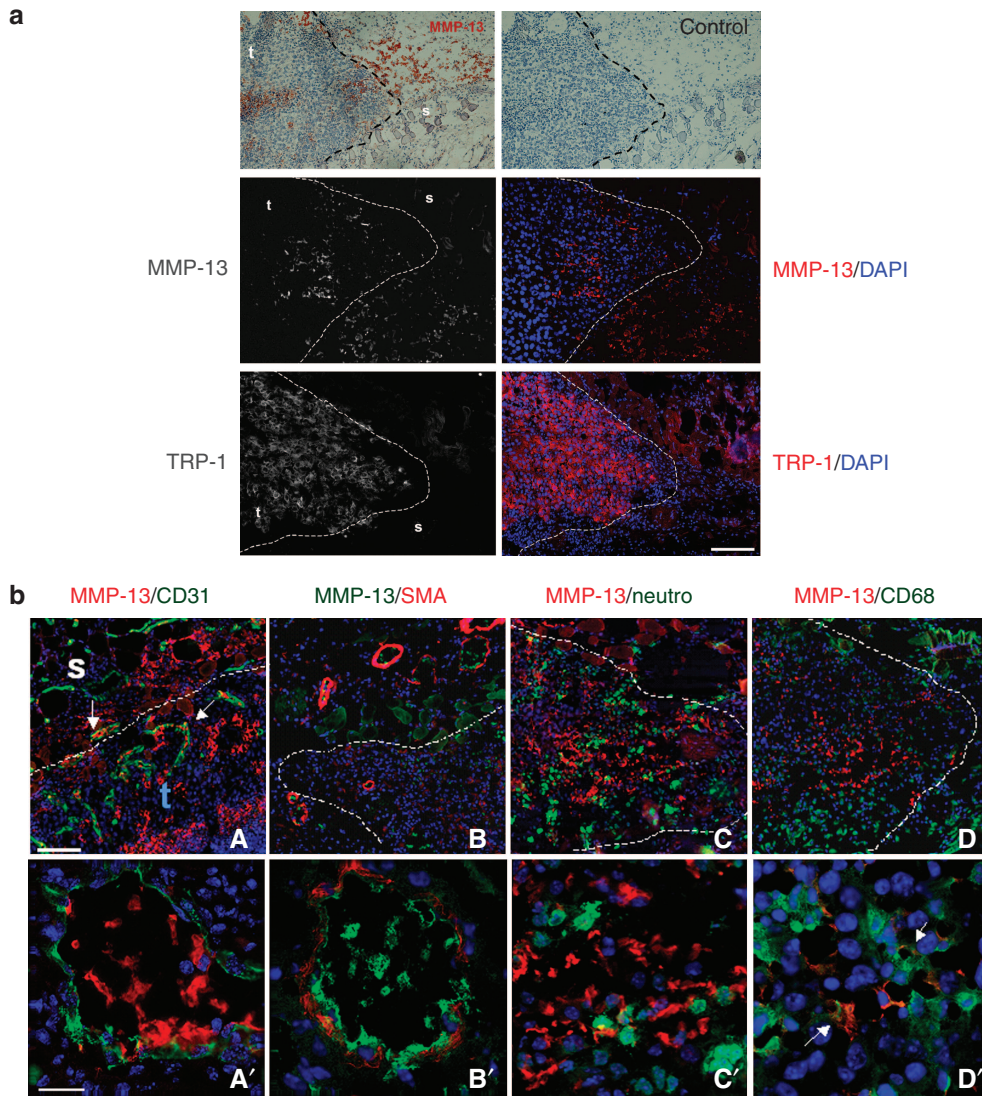
Figure 2. **Matrix metalloproteinases (MMP)-13 is expressed within the tumor and in peritumoral cells.** (**a**) Analysis of MMP-13 (red) and TRP-1 (tyrosinase-related protein-1, red) expression by immunohistochemistry in B16F1 tumors developed in wild-type animals. Black and white pictures of single MMP-13 and TRP-1 staining are shown on the right. Cellular nuclei are stained in blue. The upper pictures represent MMP-13 and control IgG immunodetection in B16F1 tumors, followed by chromogenic development. MMP-13-positive areas are shown in red. t, tumor; s, stroma. MMP-13 is detected in the peritumoral stroma, as shown by both staining methods, and within the periphery of the tumor mass. Scale bar $= 100 \mu m$. (**b**) Immunostaining of MMP-13 (red, only in **B** it is green) in the tumors of wild-type animals. **A**, counterstaining of blood vessels (CD31, green); **B**, smooth muscle actin-positive cells (SMA, red); **C**, neutrophils (neutro, green), and **D**, macrophages (CD68, green). MMP-13-positive CD31 and CD68 cells are indicated by the white arrows. Blue stain corresponds to nuclei. The lower microphotographs, A'–D' are details of the above shown confocal images (scale bar $= 100 \mu m$ A–D; scale bar $= 15 \mu m$ A'–D').

MMP-13 expression may contribute to both neo-angiogenesis and infiltration by macrophages during tumor development.

Presently it is unclear which type of tumor-associated macrophage expresses MMP-13. As the tumor growth was consistently impaired in mmp13$^{-/-}$ mice and was already visible as early as day 4 post-injection, it is conceivable that either angiogenesis and macrophage homing or phenotypic differentiation or altogether might be altered at this early time point.

Analysis of macrophage (CD68 positive) as well as neutrophil infiltration in day 4 tumors of mmp13$^{-/-}$ and WT mice, failed to show any remarkable difference in cell density and homing (Figure 4). Similar data were observed with leukocytes (data not shown). On the contrary, analysis of CD31 positive vessels in tumors showed a strong reduction of vessel density in the peritumoral areas of mmp-13$^{-/-}$ at day 4 (Figure 5). In addition, in the absence of host-derived MMP-13 a dramatic decrease in vessels penetrating into the peripheral tumor area was observed. However, few intratumoral CD31 positive vessels were still present (Figure 5a, tumor margin is marked by a dotted line).

In addition, quantification of number of CD31 and LYVE-stained vessels at day 4 of melanoma development, confirmed that density of blood (Figure 5b) but not lymphatic vessels (data not shown) was significantly decreased in mmp-13$^{-/-}$ animals bearing B16 tumors ($P < 0.0001$). Furthermore,
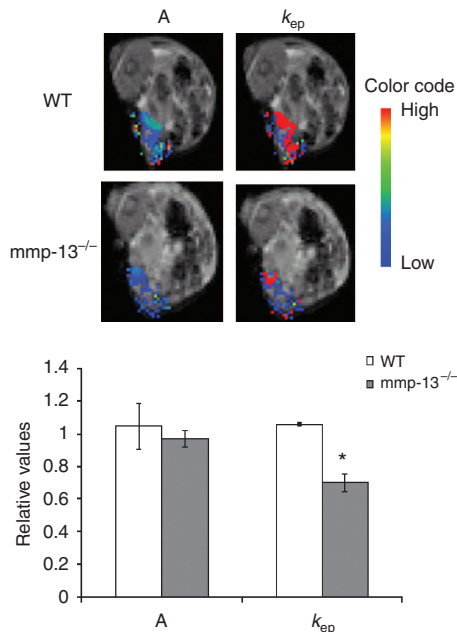
a

b

	Lung	Lymph node	Liver	Brain	Heart
WT	6/20 30%	5/20 25%	2/20 10%	6/20 30%	8/20 40%
mmp-13$^{-/-}$	6/34 17.6%	7/34 20.6%	1/34 2.9%	4/34 11.8%	0/34 0%

Figure 3. Kinetics of the growth of B16F1 grafts and metastasis in wild-type and mmp-13$^{-/-}$ animals. (**a**) Tumor sizes (mm^3) were measured as function of time after intradermal injection of B16 melanoma cells in wild-type (WT) and mmp-13$^{-/-}$ mice. Data were expressed as average ± SEM; n represents the number of animals per group. Hematoxilin-eosin staining of sections from tumors at day 4 post-injection is shown (when the divergence of tumor growth is most significant) Scale bar = 100 μm. **$P < 0.0057$ and *$P < 0.01$. (**b**) Reverse transcription–PCR amplification of the GFP gene was used to detect B16F1 melanoma cells in the various dissected organs at day 11 after intradermal injection of B16F1 melanoma cells in wild-type (wt) and mmp-13$^{-/-}$ mice. Numbers of positive amplified signals are expressed as number of positive animals on the total number analyzed and below as percentage of the analyzed organs.

while MMP-13 expression was absent in mmp-13$^{-/-}$ animals in tumor and stroma, in WT animals strong expression is appearing in the tumor and peritumoral stroma concomitantly with the induction of angiogenic response (Figure 5a, white arrows).

Lack of MMP-13 inhibits tumor growth and invasion by inhibiting *de novo*-induced tumor angiogenesis

Vascular leakage is present in pathological angiogenesis as observed in retinopathy and also during tumor development (Timar *et al.*, 2001). To analyze whether reduction in blood vessel density also results in alteration of intra-tumoral blood volume and vessel permeability, we have used *in vivo* dynamic contrast-enhanced magnetic resonance imaging (DCE-MRI) according to a pharmacokinetic two-compart-

Figure 4. Neutrophil and macrophages are recruited around the tumors. Immunostaining of neutrophils and macrophages CD68 (both in green) of cryosections from B16F1 skin tumors from mmp-13$^{-/-}$ and wild-type (WT) animals. Scale bar = 100 μm.

a

b

Figure 5. Angiogenesis and tumor infiltration. (**a**) Analysis of angiogenesis and vascularization of B16F1 grafts at day 4 post-injection of wild-type (WT) and mmp-13$^{-/-}$ animals. Immunostaining of CD31-positive endothelial cells (green) and MMP-13 (red) positive peritumoral and tumor areas. White arrows indicate areas where MMP-13 is expressed. Nuclei were stained by DAPI (blue). The dotted line delineates the tumor. On the right panel, black and white microphotographs of MMP-13 immunodetection are shown. Scale bar = 100 μm. (**b**) Quantification of stromal angiogenesis and tumor vascularization confirms the reduced angiogenic response in the entire tissue, bars represent the average number of blood vessels ± SEM of three 100 × magnification fields per section taken in the middle, half, and end of the tumor from each of four animals. ***$P < 0.001$.

ment model. This method described by Brix *et al.* (1991) allows to determine the parameters Amplitude, A, which is a measure of blood volume and exchange rate constant, k_{ep}, which is associated with vessel permeability in animals

Figure 6. Stromal depletion of matrix metalloproteinases (MMP)-13 leads to a reduction in DCE-MRI parameters A and k_{ep}. From dynamic contrast-enhanced magnetic resonance imaging (DCE-MRI) the parameters amplitude (A) and exchange rate constant (k_{ep}) were assessed of the tumors developed in wild-type (WT) and mmp-13$^{-/-}$ mice at day 6 post-injection. In the upper panel axial MRI images of mice are shown with color maps of parameters analyzed in the tumors are shown. Tumors developed in mmp-13$^{-/-}$ animals showed significantly lower k_{ep} values (*$P<0.02$; surrogate parameter for vessel permeability) than the WT control tumors whereas no significant difference in the parameter A (surrogate parameter for blood volume) was detected (left graph).

carrying grafted tumors. In inoculated WT animals the parameters *A* (NS), which is a surrogate parameter for blood volume and k_{ep} ($P<0.02$), which is associated with vessel permeability, were decreased in tumors of mmp-13$^{-/-}$ mice compared with controls (Figure 6). Thus, the observed reduction in blood vessel permeability together with the reduced CD31 staining observed in the tumor periphery (Figure 5) collectively show a reduction of angiogenetic processes around the tumors in mmp-13$^{-/-}$ mice.

DISCUSSION

Expression of proteolytic enzymes during the progression of cancer has been consistently associated with poor prognosis in a variety of cancers. Matrix metalloproteinases are believed to mediate tumor invasion through several mechanisms, including activation of other enzymes, processing of matrix components to modulate cell migration, and release of bioactive factors bound to the ECM. In addition, crosstalk between tumor and stromal cells is known to also induce protease production by one or both cell types (Gallagher *et al.*, 2005; Zigrino *et al.*, 2005). However, the molecular mechanisms by which these enzymes contribute to the progression of this tumor *in vivo* are still a matter of investigation.

Of all collagenolytic enzymes only expression of MMP-1 and MMP-13 mRNA has been found to correlate with

melanoma progression and early metastasis (Airola *et al.*, 1999; Nikkola *et al.*, 2001; Kuivanen *et al.*, 2005), and expression of MMP-13 is believed to promote tumor development in other type of cancers (Kahari *et al.*, 1998; Nielsen *et al.*, 2001; Zhang *et al.*, 2008). The cellular source and role of MMP-13 appears to be different depending on the type of tumor analyzed.

In breast cancer, Zhang *et al.* (2008) suggested that only tumor-derived, but not stromal fibroblast-derived, MMP-13 correlated with aggressive tumor phenotypes. In agreement, in invasive and metastatic human skin tumors, MMP-13 expression was predominantly confined to the tumor cells (Airola *et al.*, 1999), whereas its expression was absent in normal dermis and benign pigmented lesions.

Conversely, in mouse models for squamous-cell carcinomas and in breast cancer xenografts, a prominent upregulation of MMP-13 was observed in the host stroma (Lafleur *et al.*, 2005; Akgul *et al.*, 2006). Consistent with these data, we could show a strong expression of mouse MMP-13 in the stroma surrounding B16F1 tumors as well as in few intratumoral cells. This is in agreement with the lack amplification of MMP-13 from tumors developed in WT animals (Figure 1), thus implying that MMP-13 is derived from tumor-infiltrating stromal cells. However, Corte *et al.* (2005) have detected MMP-13 in tumor cells in 30% of *in situ* melanomas. Thus, it is possible that expression of MMP-13 by stromal cells may be necessary to direct toward a malignant phenotype in a specific and narrow time frame. In agreement with this hypothesis are the data showing that stroma-derived MMP-13 was induced only when a differentiated human premalignant epithelium shifted to a malignant and invasive tumor phenotype (Vosseler *et al.*, 2005).

On the basis of these data we have used a mouse model where expression of host-derived MMP-13 is abolished in order to identify specific functions for this protease during melanoma development *in vivo*. Indeed, depletion of MMP-13 resulted in a significant reduction in tumor growth and metastasis formation. The complete lack of metastasis to the heart is presently not understood and suggests a specific role of MMP-13 in modifying adhesion molecules, homing receptors, or the matrix of this tissue. Ongoing proteomic analysis may unravel the mechanisms of this finding. When analyzing the kinetics of tumor growth in the WT *versus* the mmp-13$^{-/-}$ animals, a clear difference in tumor growth was visible already at earlier time points thus indicating a critical role of MMP-13 in the early stage of tumor formation. For the progression from a benign to a malignant phenotype, melanoma requires cross communication with stroma as well as the creation of an inflammatory milieu (Zigrino *et al.*, 2005). In the present model of melanoma, the influence of neutrophils, macrophages, and leukocytes (not shown) was not altered suggesting that influx of inflammatory cells does not depend on MMP-13 and that modulation of the inflammatory reaction is not responsible for the observed differences in tumor growth.

In addition to a significant reduction of vessel formation, infiltration of blood vessels into the tumor mass and thus tumor vascularization was dramatically reduced in the

absence of host MMP-13. Zijlstra *et al.* (2004) have identified MMP-13 as one of the collagenases responsible for collagen remodeling associated with angiogenesis, thus implying that MMP-13 in angiogenesis may be necessary for cellular migration rather than participating in the VEGF/VEGFR cascade. In agreement with these data we have failed to see any significant difference in the levels of VEGF in extracts from the tumors (data not shown).

The crucial role of MMP-13 in promoting and maintaining angiogenesis is further supported by the localization of MMP-13 in close proximity to newly formed blood vessels. New blood vessel formation in a chorioallantoic membrane assay is dependent on the collagenolytic activity of macrophage-derived chMMP-13 (Zijlstra *et al.*, 2004). In addition, macrophages have also been shown to produce MMP-13, which they use to resorb the interstitial matrix and successfully remodel the fibrotic liver (Fallowfield *et al.*, 2007). Other cells implicated in MMP-13 production are neutrophils, which were shown to secrete MMP-9 and MMP-13 thereby modulating angiogenesis, by remodeling the ECM (Obermueller *et al.*, 2004). We have detected both cell types in the peritumoral stroma of melanoma grafts, and MMP-13 production was detected in only a few macrophages.

The MMP-13 expression colocalized with CD31 staining cells, strongly suggesting that endothelial cells are an important cellular source of this protease. This finding is supported by the observation that MMP-13 in endothelial cells is polarized toward the vessel lumina thus indicating a secretory activity.

Interestingly, active MMP-13 was found in serum in melanoma patients (Nikkola *et al.*, 2005). Furthermore, serum levels of MMP-13 have been associated with severity of systemic sclerosis (Asano *et al.*, 2006). However, whether this may represent a clearing path for depletion of the enzyme or a distribution way is presently unclear. Further studies are ongoing to clarify whether the secretion of MMP-13 may contribute to metastasis formation.

Tumor vessels are characterized by their disorganized structure with a low maturity and a high degree of vessel permeability (Metheny-Barlow and Li, 2003). In mmp-13$^{-/-}$ mice, vessel permeability was reduced as suggested by the MRI measurements, where a significant k_{ep} was observed. It is possible that not all vessels visualized in tumors by immunostaining are really functional and perfused. Thus, the blood volume may be equal in tissues with few large vessels as compared with those with many small vessels.

However, decreased blood vessel density during tumor growth in mmp-13$^{-/-}$ mice paralleled the decreased blood vessel permeability *in vivo*, as detected by MRI of tumor-bearing animals. Therefore, we can assume that reduced perfusion in mmp-13$^{-/-}$ mice is the result of reduced angiogenesis. In addition, reduced angiogenesis and most likely reduced proteolysis in the proximity of these vessels may account for the reduced percentage of metastasis through the hematogenous pathway. As we failed to see differences in the levels of several proangiogenetic factors (for example, VEGF, bFGF, IL-1, data not shown) in the extracts from tumors of WT and mmp-13$^{-/-}$ animals, we hypothesize

that lack of matrix proteolysis from ''invading'' endothelial cells may be responsible for reduced angiogenesis and intratumoral vascularization. The reduced availability of vessels may also lead to reduction of tumor cells spreading in the organism.

These data together implicate MMP-13 in melanoma growth and reveal an unexpected role for this protease in organ-specific metastasis of melanoma cells and in pathological angiogenesis.

MATERIALS AND METHODS

Transgenic animals

The mmp-13$^{-/-}$ mice in a C57BL/6 background (backcrossed for 10 generations) were generated and genotyped by PCR and Southern blot as described earlier (Hartenstein *et al.*, 2006). All animal experiments were performed in accordance with the Institutional Guidelines.

Tumorigenicity assay *in vivo*

B16-F1 cells (1×10^6) in 100 µl were injected intradermally into the flank of 6- to 8-week-old WT (floxed mmp-13$^{-/-}$) and mmp-13$^{-/-}$ littermate mice. Tumor size was measured every 2 days using a precision calliper up to 14 days. Tumor volume was calculated by multiplying length, width, depth and expressed as average ± SEM. The animal experiments have been approved by the local veterinary authority (NRW authorization 50.203.2-K 37a, 20/05).

RT–PCR analysis

Total DNase-treated RNA from the various organs was prepared using the RNAeasy Fibrous tissue Kit following the manufacturer's instructions (Qiagen, Germany). RT–PCR was performed according to the manufacturer's instructions (REDTaq ReadyMix PCR Reaction Mix, Sigma, Taufkirchen, Germany). Briefly, 1 µg RNA was reverse transcribed using oligo dT as primer in a total volume of 25 µl. A volume of 2 µl of the cDNA was used to amplify specific transcripts by PCR. Primers for the amplification of murine MMP-13 and MMP-14 were elsewhere described (Kim *et al.*, 2000). The following primers were used for amplification of murine S26: 5′-AATGTGCAGCCC ATTCGCTG and 5′-CTTCCGTCCTTACAAAACGG (NM013765); GFP: 5′-ACCCCGACCACATGAAGCAGC and 5′-CGTTGGGGTC TTTGCTCAGGG. PCRs were performed on 1 µl cDNA for 35–38 cycles (within the linear range of amplification): denaturation (94°C, 1 minute), annealing (56°C, 1 minute), and extension (72°C, 1 minute). The products were then analyzed on 2% agarose gels in Tris-borate-EDTA.

Histological analysis and indirect immunofluorescence staining of skin sections

Tumor samples at the indicated time points were snap-frozen in optimal-cutting-temperature compound (O.C.T. Tissue Tec) and cryosectioned (7 µm). Immunostaining to detect MMP-13 (Santa Cruz Biotechnology, Heidelberg, Germany), melanoma antigen (tyrosinase-related protein-1, TRP-1; Santa Cruz Biotechnology), smooth muscle actin (SMA; Cy3-conjugated; Sigma), macrophages (CD68) and neutrophils (anti-neutrophils; Serotec, Düsseldorf, Germany), endothelial cells (CD31, Pharmingen, Heidelberg, Germany), and polymorphonuclear cells (CD45) was performed as described earlier (Hartenstein *et al.*, 2006) and examined

with a Nikon Eclipse 800 fluorescence microscope equipped with a DXM1200 digital camera. In addition, anti-MMP-13 antibodies were also detected using a peroxidase-conjugated secondary antibody and chromogenic development using Envision system (DAKO).

Analysis of blood vessel density

For assessment of the tumor vessel count, different fields in each section (taken from central, intermediate and peripheral part of the tumor) were examined. Quantification was performed using ImageJ software (http://rsb.info.nih.gov/ij). The mean number of CD31-positive vessels was calculated from three $100 \times$ magnification fields per section (from five different sections per animal) of four different animals per time point according to the published protocols (Eikesdal *et al.*, 2008; Xue *et al.*, 2008).

Dynamic contrast-enhanced MRI

Dynamic contrast-enhanced MRI was performed on a clinical 1.5-Tesla whole-body MRI system (Siemens Symphony, Erlangen, Germany) using a custom-made radiofrequency coil (animal resonator) (Kiessling *et al.*, 2003). The MRI sequence was a T1-weighted inversion recovery turbo flash sequence (TR 13 ms, TE 5.3 ms, TI 300 ms, slice thickness 2 mm, FOV 60×60 mm^2, Matrix 128, orientation axial). For examination and catheterization, WT or mmp-13$^{-/-}$ mice (five per group) bearing a 6 days old B16 melanoma graft, were anesthetized by inhalation of a mixture of isoflurane (1.5%), N$_2$O (35%), and O$_2$ (60%). A tail vein was catheterized using a 30-gauge needle connected to a 10-cm-long phycoerythrin 10 polyethylene catheter (Portex, Medic-Eschmann, Germany) filled with 10 µl of 0.9% NaCl. The needle was fixed on the mouse tail with superglue. The distal end of the catheter was connected with a 1-ml tuberculin syringe, both containing MRI contrast media (gadolinium diethylenetriaminepentaacetic acid, Gd-DTPA; Magnevist Schering, Berlin, Germany). MRI contrast media (0.1 mmol Gd-DTPA per kg diluted in 0.9% NaCl to a total volume of 100 µl) was injected manually within 5 seconds into the tail vein of mice.

Analysis of the dynamic data was based on the pharmacokinetic two-compartment model of Brix *et al.* (1991), where compartment 1 is defined as the intravascular extracellular space and compartment 2 as the extravascular extracellular space. After infusion of the contrast agent, an exchange of contrast agent between both compartments is assumed, described by the exchange rate constant k_{ep}, which is closely related to vessel permeability. Another commonly used functional parameter of the Brix model is the amplitude *A*. This parameter reflects the relative change in signal intensity during contrast media application and is a surrogate parameter for blood volume.

Statistics

Two-tailed Student's *t*-test was used for data analysis, with $P < 0.05$ considered to be statistically significant.

CONFLICT OF INTEREST

The authors state no conflict of interest.

REFERENCES

Airola K, Johansson N, Kariniemi AL, Kahari VM, Saarialho-Kere UK (1997) Human collagenase-3 is expressed in malignant squamous epithelium of the skin. *J Invest Dermatol* 109:225–31

Airola K, Karonen T, Vaalamo M, Lehti K, Lohi J, Kariniemi AL *et al.* (1999) Expression of collagenases-1 and -3 and their inhibitors TIMP-1 and -3 correlates with the level of invasion in malignant melanomas. *Br J Cancer* 80:733–43

Akgul B, Pfefferle R, Marcuzzi GP, Zigrino P, Krieg T, Pfister H *et al.* (2006) Expression of matrix metalloproteinase (MMP)-2, MMP-9, MMP-13, and MT1-MMP in skin tumors of human papillomavirus type 8 transgenic mice. *Exp Dermatol* 15:35–42

Asano Y, Ihn H, Kubo M, Jinnin M, Mimura Y, Ashida R *et al.* (2006) Clinical significance of serum levels of matrix metalloproteinase-13 in patients with systemic sclerosis. *Rheumatology (Oxford)* 45:303–7

Brix G, Semmler W, Port R, Schad LR, Layer G, Lorenz WJ (1991) Pharmacokinetic parameters in CNS Gd-DTPA enhanced MR imaging. *J Comput Assist Tomogr* 15:621–8

Corte MD, Gonzalez LO, Corte MG, Quintela I, Pidal I, Bongera M *et al.* (2005) Collagenase-3 (MMP-13) expression in cutaneous malignant melanoma. *Int J Biol Markers* 20:242–8

Eikesdal HP, Sugimoto H, Birrane G, Maeshima Y, Cooke VG, Kieran M *et al.* (2008) Identification of amino acids essential for the antiangiogenic activity of tumstatin and its use in combination antitumor activity. *Proc Natl Acad Sci USA* 105:15040–5

Fallowfield JA, Mizuno M, Kendall TJ, Constandinou CM, Benyon RC, Duffield JS *et al.* (2007) Scar-associated macrophages are a major source of hepatic matrix metalloproteinase-13 and facilitate the resolution of murine hepatic fibrosis. *J Immunol* 178:5288–95

Gallagher PG, Bao Y, Prorock A, Zigrino P, Nischt R, Politi V *et al.* (2005) Gene expression profiling reveals cross-talk between melanoma and fibroblasts: implications for host-tumor interactions in metastasis. *Cancer Res* 65:4134–46

Hartenstein B, Dittrich BT, Stickens D, Heyer B, Vu TH, Teurich S *et al.* (2006) Epidermal development and wound healing in matrix metalloproteinase 13-deficient mice. *J Invest Dermatol* 126:486–96

Itoh T, Tanioka M, Yoshida H, Yoshioka T, Nishimoto H, Itohara S (1998) Reduced angiogenesis and tumor progression in gelatinase A-deficient mice. *Cancer Res* 58:1048–51

Itoh Y, Binner S, Nagase H (1995) Steps involved in activation of the complex of pro-matrix metalloproteinase 2 (progelatinase A) and tissue inhibitor of metalloproteinases (TIMP)-2 by 4-aminophenylmercuric acetate. *Biochem J* 308(Part 2):645–51

Kahari VM, Johansson N, Grenman R, Airola K, Saarialho-Kere U (1998) Expression of collagenase-3 (MMP-13) by tumor cells in squamous cell carcinomas of the head and neck. *Adv Exp Med Biol* 451:63–8

Kiessling F, Heilmann M, Vosseler S, Lichy M, Krix M, Fink C *et al.* (2003) Dynamic T1-weighted monitoring of vascularization in human carcinoma heterotransplants by magnetic resonance imaging. *Int J Cancer* 104:113–20

Kim MH, Kitson RP, Albertsson P, Nannmark U, Basse PH, Kuppen PJ *et al.* (2000) Secreted and membrane-associated matrix metalloproteinases of IL-2-activated NK cells and their inhibitors. *J Immunol* 164:5883–9

Kuivanen T, Ahokas K, Virolainen S, Jahkola T, Holtta E, Saksela O *et al.* (2005) MMP-21 is upregulated at early stages of melanoma progression but disappears with more aggressive phenotype. *Virchows Arch* 447:954–60

Kurschat P, Wickenhauser C, Groth W, Krieg T, Mauch C (2002) Identification of activated matrix metalloproteinase-2 (MMP-2) as the main gelatinolytic enzyme in malignant melanoma by *in situ* zymography. *J Pathol* 197:179–87

Lafleur MA, Drew AF, de Sousa EL, Blick T, Bills M, Walker EC *et al.* (2005) Upregulation of matrix metalloproteinases (MMPs) in breast cancer

xenografts: a major induction of stromal MMP-13. *Int J Cancer* 114:544–54

Loffek S, Zigrino P, Angel P, Anwald B, Krieg T, Mauch C (2005) High invasive melanoma cells induce matrix metalloproteinase-1 synthesis in fibroblasts by interleukin-1alpha and basic fibroblast growth factor-mediated mechanisms. *J Invest Dermatol* 124:638–43

Madlener M, Parks WC, Werner S (1998) Matrix metalloproteinases (MMPs) and their physiological inhibitors (TIMPs) are differentially expressed during excisional skin wound repair. *Exp Cell Res* 242:201–10

Metheny-Barlow LJ, Li LY (2003) The enigmatic role of angiopoietin-1 in tumor angiogenesis. *Cell Res* 13:309–17

Nielsen BS, Rank F, Lopez JM, Balbin M, Vizoso F, Lund LR *et al.* (2001) Collagenase-3 expression in breast myofibroblasts as a molecular marker of transition of ductal carcinoma *in situ* lesions to invasive ductal carcinomas. *Cancer Res* 61:7091–100

Nikkola J, Vihinen P, Vlaykova T, Hahka-Kemppinen M, Kahari VM, Pyrhonen S (2001) High collagenase-1 expression correlates with a favourable chemoimmunotherapy response in human metastatic melanoma. *Melanoma Res* 11:157–66

Nikkola J, Vihinen P, Vuoristo MS, Kellokumpu-Lehtinen P, Kahari VM, Pyrhonen S (2005) High serum levels of matrix metalloproteinase-9 and matrix metalloproteinase-1 are associated with rapid progression in patients with metastatic melanoma. *Clin Cancer Res* 11:5158–66

Obermueller E, Vosseler S, Fusenig NE, Mueller MM (2004) Cooperative autocrine and paracrine functions of granulocyte colony-stimulating factor and granulocyte-macrophage colony-stimulating factor in the progression of skin carcinoma cells. *Cancer Res* 64:7801–12

Stickens D, Behonick DJ, Ortega N, Heyer B, Hartenstein B, Yu Y *et al.* (2004) Altered endochondral bone development in matrix metalloproteinase 13-deficient mice. *Development* 131:5883–95

Timar J, Dome B, Fazekas K, Janovics A, Paku S (2001) Angiogenesis-dependent diseases and angiogenesis therapy. *Pathol Oncol Res* 7:85–94

Vosseler S, Mirancea N, Bohlen P, Mueller MM, Fusenig NE (2005) Angiogenesis inhibition by vascular endothelial growth factor receptor-2 blockade reduces stromal matrix metalloproteinase expression, normalizes stromal tissue, and reverts epithelial tumor phenotype in surface heterotransplants. *Cancer Res* 65:1294–305

Wandel E, Grasshoff A, Mittag M, Haustein UF, Saalbach A (2000) Fibroblasts surrounding melanoma express elevated levels of matrix metalloproteinase-1 (MMP-1) and intercellular adhesion molecule-1 (ICAM-1) *in vitro*. *Exp Dermatol* 9:34–41

Westermarck J, Kahari VM (1999) Regulation of matrix metalloproteinase expression in tumor invasion. *FASEB J* 13:781–92

Wilson CL, Heppner KJ, Labosky PA, Hogan BL, Matrisian LM (1997) Intestinal tumorigenesis is suppressed in mice lacking the metalloproteinase matrilysin. *Proc Natl Acad Sci USA* 94:1402–7

Xue Y, Cao R, Nilsson D, Chen S, Westergren R, Hedlund EM *et al.* (2008) FOXC2 controls Ang-2 expression and modulates angiogenesis, vascular patterning, remodeling, and functions in adipose tissue. *Proc Natl Acad Sci USA* 105:10167–72

Zhang B, Cao X, Liu Y, Cao W, Zhang F, Zhang S *et al.* (2008) Tumor-derived matrix metalloproteinase-13 (MMP-13) correlates with poor prognoses of invasive breast cancer. *BMC Cancer* 8:83

Zigrino P, Loffek S, Mauch C (2005) Tumor-stroma interactions: their role in the control of tumor cell invasion. *Biochimie* 87:321–8

Zijlstra A, Aimes RT, Zhu D, Regazzoni K, Kupriyanova T, Seandel M *et al.* (2004) Collagenolysis-dependent angiogenesis mediated by matrix metalloproteinase-13 (collagenase-3). *J Biol Chem* 279:27633–45